Mine Water Environ (2011) 30:113–126
DOI 10.1007/s10230-011-0146-4

TECHNICAL ARTICLE

# Drainage at Abandoned Mine Sites: Natural Attenuation of Contaminants in Different Seasons

**Rosa Cidu · Franco Frau · Stefania Da Pelo**

Received: 15 December 2010 / Accepted: 9 March 2011 / Published online: 22 March 2011


**Abstract** Since 1996, hydrogeochemical surveys have been carried out in the abandoned Montevecchio Pb-Zn mining district (Sardinia, Italy), where mine drainages discharge directly into the local streams, to investigate variations in the aqueous occurrence of contaminants. Natural attenuation in dissolved contaminants occurs downstream of the abandoned mines. Iron is removed first (about 2 km downstream); lead, aluminum, and copper follow (about 4 km downstream). Other metals, such as zinc, cadmium, nickel, and rare earth elements, decrease further downstream. At high flow, natural attenuation is mainly due to dilution by rainwater. At low flow, natural attenuation processes are dominated by solid phase precipitation, efflorescent salt formation due to evaporation, and dilution by uncontaminated surface and/or groundwater inflow. Overall, concentrations of sulphate, Zn, Cd, Pb, Cu, Ni, and Co were less in 2010 than in 1996. The concentrations of dissolved sulphate and metals are lowest when the water is less acidic. However, despite ongoing natural attenuation, very high concentrations of toxic metals continue to be observed 15 years after the underground workings flooded. The amount of contaminants reaching the Marceddì lagoon increases as runoff increases following heavy rains.

**Keywords** Italy · Metal dispersion · Mine closure · Mine water · Rebound · REE · Sardinia

R. Cidu (✉) · F. Frau · S. Da Pelo
Department of Earth Sciences, Cagliari University,
via Trentino 51, 09127 Cagliari, Italy
e-mail: cidur@unica.it

## Introduction

Environmental contamination at historical mining sites have been documented in Europe (e.g. Gandy and Younger 2007; Navarro et al. 2008; Wolkersdorfer and Bowell 2005) and elsewhere (e.g. Cherry et al. 2001; Lim et al. 2008; Ren et al. 2009). Past mining often affects aquatic systems in the mine district. Contamination levels in mine drainages depend on several factors, such as climate, hydrology, structural geology, composition of ore deposits, and host rocks in the mining region (e.g. Dold and Fontboté 2001). In river systems affected by mine drainage, contaminant concentrations in water and sediment tend to decrease downstream of pollution sources. These patterns have been attributed to both hydrodynamic and chemical processes (Hudson-Edwards et al. 1996). In some cases, metal and metalloid contents have been attenuated to near-background concentrations without human intervention (Berger et al. 2000; Chapman et al. 1983; Kimball et al. 2007). These studies indicate that relevant physical, chemical, and/or biological reactions can contribute to attenuation processes.

In Sardinia (Italy), a long history of metalliferous mining has left a legacy of abandoned mines and spoil heaps. Some of these old mines in the ore fields of Montevecchio are sources of highly polluted acid drainage due to the oxidative weathering of sulphide minerals. In this paper, we report: (1) variations occurring in the chemical composition of mine drainages since mine closure at Montevecchio, and (2) natural attenuation of contaminants downstream of mining-related sources of contamination. Understanding the processes that control the extent and dispersion of contaminants away from the abandoned mines could help to reduce adverse effects at active mining sites and aid the remediation of contamination from historical mining activities.

## Study Area

The Montevecchio study area is located in the Arburese mining district (SW Sardinia). The Pb-Zn vein ores are mainly galena and sphalerite. Quartz, pyrite, marcasite, and other sulphide minerals are associated with them. The ores, hosted in silicate-dominant rocks, were exploited intensively from 1850 to 1990. Underground workings extended in a system of overlapping galleries to a depth of 600 m below ground level. Pb-Zn production peaked in the mid-1900s. A subsequent fall in base metal prices and increasing labour costs led to the closure of these Pb-Zn mines during the 1970–1990 period.

Figure 1 shows the location of abandoned mines, flotation plants, and tailings in the Arburese mining district. Mine discharges have been observed since 1995, following the cessation of dewatering and the flooding of the underground workings. These contaminated waters discharge directly into the local streams. Other sources of contaminants include flotation tailings retained behind the Piccalinna dam and waste rock dumps located nearby the mine site. Part of the mining-related residues has been transported downstream of the mine and deposited on river banks in the plain (Fig. 1).

Climate in Sardinia is characterized by long periods of heat and drought, usually extending from May to September, interrupted by relatively short rainy periods, with occasional heavy rain events that have been occurring more frequently during the last decade. Mean rainfall in the study area ranges from 400 mm per year near the coast to 700 mm per year inland, with a mean of 50 rainy days per year. The mean annual temperature is 15°C (RAS 1998).

## Materials and Methods

### Solid Samples

Solid samples were collected for this study during a dry period in September 2008. They included: efflorescence and ochre samples precipitating from seeps at the base of the Piccalinna dam (SP1a-d and SP2); solid materials precipitating at mine drainage outflows (Ad1); stratified aged precipitates (Ad2 and AdR1), and; solid materials precipitating from stream water (SS10). Solid samples were stored in doubly sealed plastic bags, dried in an oven at 40°C for 24 h and immediately analyzed. X-ray powder diffraction (XRD) patterns for mineralogical characterization were

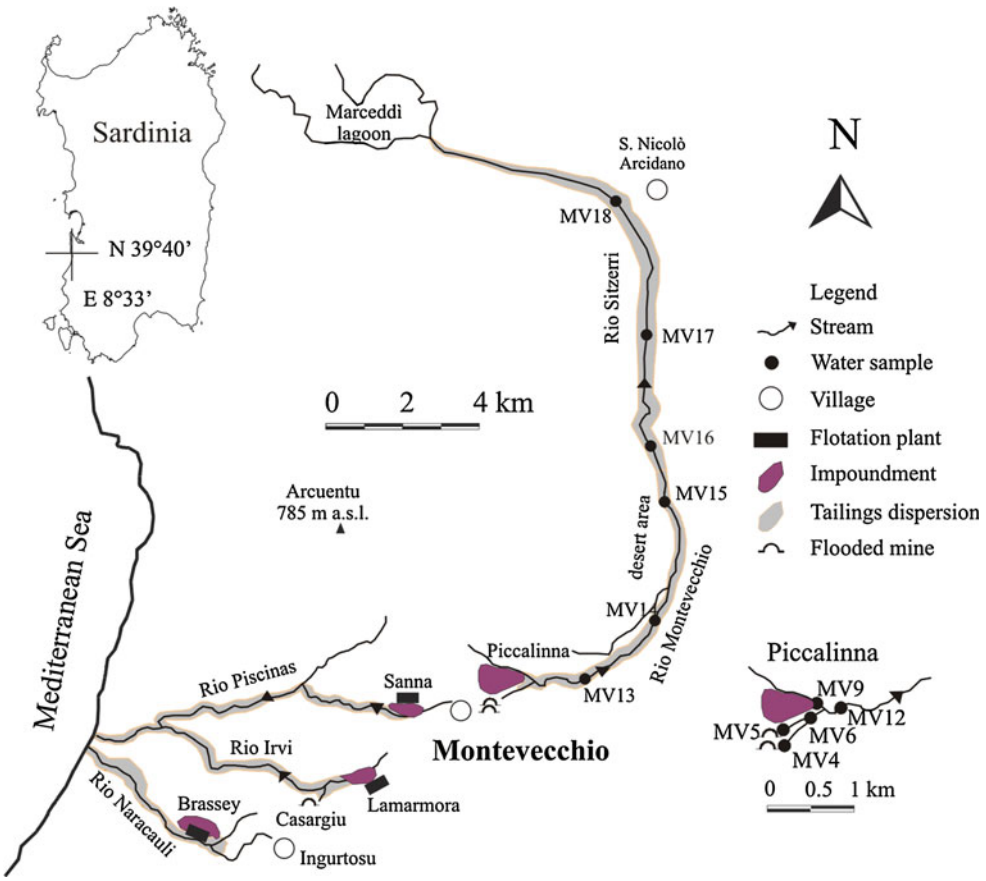


**Fig. 1** Map showing the Montevecchio mining district and location of water samples

collected in the 3–70° $2\theta$ angular range on an automated Panalytical X'pert Pro diffractometer with Ni-filter monochromatized Cu-K$\alpha$1 radiation ($\lambda = 1.54060$ Å), operating at 40 kV and 40 mA, using the X'Celerator detector in scanning mode with PSD length of 2.022°. X-ray pattern treatment was carried out by Panalytical High Score software and consisted of smoothing, K$\alpha$2 stripping, and peak search. This final step finds peak positions by detecting the minima from the second derivative of the diffractogram.

For wet analyses of selected metals and arsenic, about 0.1 g of each sample was accurately weighed, transferred into a clean PFA vessel, and digested in a CEM—MDS 2100 microwave in a mixture of 2 mL $H_2O$ (Milli-Q® ultrapure water), 1.5 mL $H_2O_2$ (30% Carlo Erba RPE), and 7 mL $HNO_3$ (68% Carlo Erba Suprapure). Solutions were diluted to 50 mL with 1% $HNO_3$ in volumetric flask, and transferred to new high density polyethylene (HDPE) bottles. Two reagent blanks and a reference standard (NIST SRM2710), prepared in the same way as the samples, were included in each digestion cycle, and several samples were run in duplicate. Metals and arsenic were determined by inductively coupled plasma—optical emission spectrometry (ICP-OES, ARL-3520B). Errors on replicate samples and replicate SRM2710 analyses were estimated to be less than 10% for all elements.

### Water Samples

Water samples have been collected in the Arburese mining district since 1996. Water samples considered in this study were collected at outflows from adits (MV4 and MV5), seeps from flotation tailings (MV9), adit waters mixed with seeps (MV6, MV8, and MV11), and stream waters (MV12 to MV18) draining the mine site.

Considering that contamination level in waters draining from abandoned mines is affected by rainfall dynamics (Kimball et al. 2007; Nordstrom 2009), water sampling was planned considering the regional climatic conditions. This paper reports on water sampling carried out at the end of summer in September 2004, and September 2008 following a severe drought, representing low flow conditions. Water samples were also collected in January 2003 during heavy rain, in March 2010, soon after the rainy season, and October 2010, at the beginning of the rainy season, to represent high flow conditions.

At the sampling site, the pH, redox potential (Eh), temperature, and alkalinity were measured; waters were filtered through 0.4 μm pore-size Nuclepore polycarbonate filters, using an all-plastic filtration assembly, into pre-cleaned HDPE bottles. Filtered aliquots were acidified on site with suprapure grade $HNO_3$ for analyses of minor and trace elements by quadrupole inductively coupled plasma—mass spectrometry (ICP-MS) and major cations by ICP-OES. A filtered aliquot was acidified on site with suprapure grade HCl for the determination of arsenic by on-line hydride generation—ICP-MS. Anions were determined by ion chromatography on a filtered, unacidified aliquot. Alkalinity was repeated in the lab by titration with HCl and pH measurement.

A certified reference solution NIST SRM1643a-e, and Teknolab Spectrascan Y and rare earth elements (REE) were used to evaluate analytical uncertainty; errors were usually found to be less than 10%. Concentration values and calculated speciation by PHREEQC (Parkhurst and Appelo 1999) reported here refer to elements determined in the aqueous fraction <0.4 μm. Geochemical modelling by PHREEQC was carried out using the 'wateq4f.dat' database implemented with the solubility constants ($K_s$ at 25°C) of two relevant Zn-minerals: hydrozincite (reaction 1) taken from the 'llnl.dat' database and hemimorphite (reaction 2) obtained by Dr. D.C. McPhail (personal communication 2010):

$$Zn_5(OH)_6(CO_3)_2 + 8H^+ \leftrightarrow 5Zn^{2+} + 2HCO_3^- + 6H_2O \quad K_s = 10^{30.3} \tag{1}$$

$$Zn_4Si_2O_7(OH)_2 \cdot H_2O + 8H^+ \leftrightarrow 4Zn^{2+} + 2H_4SiO_4 + 2H_2O \quad K_s = 10^{21.8} \tag{2}$$

## Results

### Characterization of Solid Materials

Mineralogy and chemistry of tailings materials at the Piccalinna impoundment were previously investigated (Da Pelo 1998; Da Pelo et al. 1996). These materials are mainly composed of fine-grained flotation tailings with quartz, siderite, ankerite, white mica, and barite as primary minerals, and pyrite, dolomite, sphalerite, and galena as minor phases. Gypsum, brochantite, and sometimes epsomite occur as secondary minerals. Other secondary minerals formed by the oxidative weathering of primary ore minerals have been documented. In particular, oxidation of: galena to cerussite, anglesite, and pyromorphite; sphalerite to hemimorphite, smithsonite, and hydrozincite, and; iron sulphides to goethite and ematite is widespread.

Table 1 reports concentration of arsenic and selected metals determined in efflorescence and precipitate materials collected in the Montevecchio area, together with mineral phases recognized by XRD. Mine drainages and seeps from flotation tailings at the outflow are characterized by orange-red precipitates (ochre). XRD analyses showed that Fe(III) can precipitate as amorphous or crystalline ferric oxyhydroxide and/or hydroxysulfate phases, such as ferrihydrite and schwertmannite, respectively.

**Table 1** Amounts of arsenic, metals and dominant minerals in solid materials collected at Montevecchio; date is expressed as months and years; concentrations of Fe, Zn, and Mn are in wt%; concentrations of other contaminants are in mg/kg

| Sample | Type[a] | Date | As | Cd | Co | Cu | Ni | Pb | Fe | Zn | Mn | $pH_w$[b] | Mineralogy[c] |
|---|---|---|---|---|---|---|---|---|---|---|---|---|---|
| SP1a | effl | 09.08 | 35 | 304 | 40 | 575 | 84 | 46 | 15.49 | 6.06 | 0.72 | | Al-Cop; Gy; Gun; Zn-Cop |
| SP1b | effl | 09.08 | <10 | 53 | 205 | 7 | 377 | 27 | <0.01 | 9.30 | 2.88 | | Boy; Szm; Stark |
| SP1c | prec | 09.08 | 30 | 155 | 27 | <5 | 59 | 6,097 | 19.45 | 3.34 | 0.82 | 3.24 | Gy |
| SP1d | prec | 09.08 | 18 | 227 | 20 | 10 | 35 | 1,601 | 23.58 | 1.55 | 0.55 | 3.24 | Gy; Hfo |
| SP2 | prec | 09.08 | 561 | 212 | 11 | 89 | <10 | 2,460 | 35.11 | 2.93 | 0.14 | 5.93 | Hfo |
| AdR1 | prec | 09.08 | <10 | 38 | <3 | 422 | <10 | 1,745 | 44.20 | 0.75 | 0.01 | 4.45 | Hfo; Goe |
| Ad1 | prec | 09.08 | <10 | 196 | <3 | 1,403 | 18 | 8,840 | 48.55 | 4.71 | 0.02 | 4.28 | Hfo; Goe |
| Ad2 | prec | 09.08 | <10 | 113 | <3 | 792 | 12 | 11,350 | 51.85 | 3.26 | 0.01 | 4.28 | Hfo; Goe |
| SS10 | prec | 09.08 | 105 | 25 | <3 | 35 | <10 | 583 | 48.35 | 0.39 | 0.05 | 3.57 | Hfo, Goe |

[a] *effl* efflorescence, *prec* precipitate, [b] $pH_w$ pH of water the precipitate is in contact with, [c] *Al-Cop* aluminocopiapite, $(Al)_{2/3}Fe_4(SO_4)_6(OH)_2{\cdot}20H_2O$, *Boy* boyleite, (Zn,Mg) $SO_4{\cdot}4H_2O$, *Goe* goethite, FeO(OH), *Gun* gunningite, (Zn,Mn) $SO_4{\cdot}H_2O$, *Gy* gypsum, $CaSO_4{\cdot}2H_2O$, *Hfo* ferrihydrite, $Fe_5O_8{\cdot}4H_2O$ and/or schwertmannite, $Fe_8O_8(OH)_6(SO_4)$, *Stark* starkeyite, $MgSO_4{\cdot}4H_2O$, *Szm* szmikite, $MnSO_4{\cdot}H_2O$, *Zn-Cop* zincocopiapite, $ZnFe_4(SO_4)_6(OH)_2{\cdot}20H_2O$

Trace amounts of goethite were also observed in the ochreous precipitates. However, goethite is unlikely to precipitate directly, and likely results from transformation of previously precipitated ferrihydrite or schwertmannite (Bigham et al. 1996; Yu et al. 1999). These minerals host variable amounts of trace metals, with Pb occurring up to 1 wt% (Table 1). Precipitation of the ochre continues on the Rio Montevecchio stream beds and has a marked influence on the chemistry of the stream water.

Efflorescent minerals produced by evaporative processes were consistently observed at the wall of the impoundment and along the river bed where the stream water flows underground, particularly in dry periods. Efflorescent minerals were often observed in complex miscellaneous assemblages and rarely as single phases. They host up to 9% of Zn and up to 380, 200, and 300 mg/kg of Ni, Co, and Cd, respectively (Table 1). Gypsum is very abundant and occurs even under wet conditions. Other abundant minerals are soluble sulphates, including epsomite and starkeyite, boyleite, gunningite, and szmikite; Zn- and Al-copiapite were also recognized (Table 1).

Newly-formed precipitates from acid mine drainage can remove metals and metalloids from solution, but the formation of soluble efflorescent salts can be a matter of environmental concern since acidity and metals are stored in the salts, which can dissolve quickly when exposed to rain and surface water, and can potentially infiltrate into groundwater (Nordstrom and Alpers 1999).

## Water Chemistry

Table 2 reports selected analytical data for this study. Waters flowing out of adits (MV4 and MV5) have low pH, zinc-sulphate dominant chemical composition, and high concentrations of iron, manganese, cadmium, lead, copper, nickel, cobalt, aluminum, yttrium, and REE. Seeps (MV9) from flotation tailings show chemical composition and metal concentrations similar to the adit waters, but are generally distinguished by low values of Eh and dissolved oxygen, and high arsenic (up to 260 μg/L).

Chemical composition and metal concentrations in the Rio Montevecchio (MV12 to MV14) and Rio Sitzerri (MV15 to MV18) surface waters draining the abandoned mine area depend on flow rates. The highest concentrations of sulphate and metals in the Rio Montevecchio waters occur in the dry season (September 2004 and 2008, Table 2). Sulphate and metal contents in the stream waters decrease with distance downstream of the abandoned mines.

## Temporal Variations in Mine Drainages

In 1973, under active mining and dewatering conditions, the water pumped out of Montevecchio had a near-neutral pH (6.2), with 2000 mg/L $SO_4$, 290 mg/L Zn, 1 mg/L Cd, and 1.2 mg/L Pb (Biddau 1978). In 1996, following mine closure and groundwater rebound, drainages from adits were acid, and dissolved concentrations of $SO_4$, Zn, Cd, and Pb were much higher than those observed under dewatering conditions (Caboi et al. 1996).

At Montevecchio, the MV4 and MV5 adits (Fig. 1) discharge drainage water from the underground workings. The flow rate at MV4 ranges from 0.1 to 2 L/s; it is generally higher at MV5 (1–10 L/s) due to input from surface drainage. Water in the two adits was dominantly of Zn-$SO_4$ composition. Figure 2 shows pH, $SO_4$, and Zn variations in the MV4 and MV5 waters, and the local monthly precipitation from 1996 to 2010. Water in the MV4 adit showed nearly constant pH (3.9 ± 0.4). The acidity produced by the oxidative weathering of sulphide minerals (especially

pyrite) has been preserved at MV4 due to the paucity of carbonate minerals in this system. The pH at MV5 varied from 3.4 to 7.4 depending on the amount of rainwater inflow. The lowest pH values at MV5 were observed when sampling was carried out after long droughts, such as in September 2008 (Table 2).

Under very acidic conditions (pH = 3.5 in 2001), mine drainage from Montevecchio showed peak concentrations of dissolved sulphate (6 g/L) and metals (mg/L): 3,000 Zn, 30 Cd, 2.4 Pb, 130 Fe, 100 Mn, 18 Al, 14 Cu, 2.8 Ni, 1.8 Co, and 2.1 ΣREE (sum from La to Lu). Speciation calculations by PHREEQC show that the most abundant species were divalent free metals (e.g. $Zn^{2+}$, $Cd^{2+}$, $Cu^{2+}$, $Mn^{2+}$, $Pb^{2+}$, and $Ni^{2+}$), the amount of which increased with increasing acidity, and aqueous complexes dominated by the sulphate ligand (e.g. $ZnSO_4°$, $CdSO_4°$, $CuSO_4°$, $MnSO_4°$, $PbSO_4°$, and $NiSO_4°$).

Dissolved Fe, Mn, Cd, Cu, Al, Pb, Ni, and Co concentrations in the MV4 drainage were generally higher than at MV5. Figure 3 shows variations of some metals in the MV4 and MV5 adit waters during the monitoring period. In both mine drainages, concentrations of metals, particularly Al and Pb, increased as pH values decreased, which is consistent with the higher mobility of these metals under more acidic conditions (Stumm and Morgan 1996). Results of hydrogeochemical surveys showed a significant decrease

**Table 2** Flow, temperature, redox potential (Eh), dissolved oxygen (DO), pH, electrical conductivity (EC), and chemical components in water samples, filtered through 0.4 μm pore size filters, collected in the Montevecchio area (nd = not determined)

| No. | Date (mm.yy) | Flow (L/s) | T (°C) | Eh (V) | DO (mg/L) | pH | EC (mS) | Ca (mg/L) | Mg (mg/L) | Na (mg/L) | K (mg/L) | $HCO_3^-$ (mg/L) | $Cl^-$ (mg/L) | $SO_4^{-2}$ (mg/L) | Fe (mg/L) | Mn (mg/L) | Zn (mg/L) |
|---|---|---|---|---|---|---|---|---|---|---|---|---|---|---|---|---|---|
| MV4 | 09.04 | 0.2 | 19 | 0.57 | nd | 4.0 | 3.7 | 220 | 84 | 41 | 12 | | 45 | 2,800 | 90 | 45 | 1,200 |
| MV4 | 09.08 | 0.1 | 20 | 0.46 | 3.3 | 4.2 | 4.0 | 190 | 70 | 42 | 10 | | 61 | 3,300 | 90 | 46 | 1,200 |
| MV4 | 12.09 | 1 | 17 | 0.73 | 8 | 3.8 | 3.5 | 164 | 71 | 42 | 7 | | 63 | 3,000 | 83 | 46 | 1,200 |
| MV4 | 03.10 | 1 | 18 | 0.44 | nd | 4.1 | 3.0 | 175 | 77 | 43 | 6 | 9 | 45 | 2,700 | 80 | 50 | 1,300 |
| MV5 | 09.04 | 0.5 | 18 | 0.74 | nd | 4.0 | 3.2 | 230 | 130 | 49 | 12 | | 48 | 2,280 | 0.5 | 36 | 750 |
| MV5 | 09.08 | 0.3 | 18 | 0.72 | 7.1 | 3.4 | 2.9 | 180 | 85 | 58 | 10 | | 83 | 2,000 | 3.6 | 27 | 550 |
| MV5 | 12.09 | 1 | 13 | 0.62 | 8 | 4.3 | 2.4 | 161 | 78 | 64 | 6 | | 77 | 1,560 | 0.5 | 19 | 500 |
| MV5 | 03.10 | 2 | 14 | 0.48 | 8.4 | 6.5 | 1.7 | 154 | 70 | 64 | 5 | 40 | 100 | 1,060 | 2.0 | 15 | 350 |
| MV5 | 10.10 | 1 | 17 | 0.57 | 7.4 | 5.0 | 2.0 | 166 | 71 | 29 | 8 | 7 | 32 | 1,620 | 0.25 | 18 | 700 |
| MV6 | 12.09 | 4 | 13 | 0.69 | 2.2 | 4.3 | 2.6 | 163 | 74 | 48 | 5 | 60 | 55 | 1,880 | 63 | 42 | 700 |
| MV6 | 03.10 | 3 | 18 | 0.69 | 1.2 | 4.3 | 2.4 | 187 | 82 | 51 | 5 | 12 | 68 | 2,000 | 60 | 40 | 750 |
| MV6 | 10.10 | 3 | 19 | 0.43 | 2.2 | 5.4 | 1.5 | 132 | 65 | 33 | 6 | 12 | 49 | 1,090 | 37 | 39 | 300 |
| MV8 | 09.08 | 1.2 | 23 | 0.58 | 6.8 | 3.5 | 4.2 | 290 | 120 | 48 | 10 | | 62 | 3,300 | 106 | 81 | 910 |
| MV9 | 09.08 | 0.01 | 26 | 0.26 | 1.7 | 6.0 | 3.5 | 440 | 210 | 40 | 20 | 85 | 47 | 2,500 | 95 | 70 | 100 |
| MV11 | 09.04 | 6 | 20 | 0.66 | nd | 3.4 | 4.2 | 400 | 220 | 60 | 18 | | 60 | 3,500 | 110 | 180 | 670 |
| MV11 | 09.08 | 1 | 27 | 0.63 | 6.3 | 3.3 | 4.0 | 380 | 200 | 60 | 20 | | 77 | 3,100 | 30 | 81 | 430 |
| MV11 | 03.10 | 6 | 15 | 0.40 | 4.4 | 6.0 | 1.6 | 150 | 76 | 47 | 5 | 17 | 58 | 1,200 | 30 | 35 | 280 |
| MV12 | 09.04 | 1 | 20 | 0.71 | nd | 3.3 | 4.2 | 420 | 240 | 66 | 19 | | 61 | 3,300 | 90 | 160 | 560 |
| MV12 | 10.10 | 5 | 19 | 0.50 | 6 | 5.1 | 1.6 | 174 | 97 | 55 | 9 | 9 | 80 | 1,100 | 8 | 27 | 140 |
| MV13 | 09.04 | 10 | 21 | 0.75 | nd | 3.3 | 3.9 | 380 | 220 | 83 | 18 | | 90 | 2,800 | 7 | 100 | 450 |
| MV13 | 09.08 | 1 | 27 | 0.65 | 5.5 | 3.4 | 4.0 | 370 | 200 | 80 | 20 | | 96 | 2,700 | 5.2 | 70 | 380 |
| MV13 | 03.10 | 7 | 20 | 0.43 | 7 | 6.2 | 1.4 | 118 | 62 | 58 | 4 | 15 | 83 | 880 | 10 | 24 | 190 |
| MV13 | 10.10 | 7 | 19 | 0.56 | 6.2 | 4.8 | 1.7 | 180 | 98 | 54 | 10 | 7 | 73 | 1,240 | 7 | 29 | 200 |
| MV14 | 09.04 | 2 | 21 | 0.72 | nd | 3.6 | 3.8 | 360 | 220 | 86 | 15 | | 92 | 2,700 | 0.5 | 100 | 440 |
| MV14 | 03.10 | 5 | 19 | 0.48 | 8 | 7.0 | 1.2 | 90 | 52 | 60 | 4 | 32 | 80 | 640 | 0.9 | 17 | 130 |
| MV15 | 09.04 | 1 | 26 | 0.55 | nd | 6.2 | 3.7 | 470 | 270 | 130 | 19 | 12 | 130 | 3,400 | 0.1 | 100 | 600 |
| MV16 | 09.04 | 1 | 24 | 0.63 | nd | 6.4 | 4.2 | 550 | 320 | 150 | 25 | 12 | 160 | 3,800 | 0.05 | 120 | 700 |
| MV16 | 10.10 | 50 | 19 | 0.57 | 8 | 6.4 | 1.7 | 190 | 94 | 57 | 9 | 14 | 73 | 1,200 | 0.03 | 30 | 230 |
| MV17 | 09.04 | 5 | 21 | 0.46 | nd | 7.6 | 1.0 | 35 | 16 | 98 | 12 | 130 | 130 | 61 | 0.07 | 0.03 | 0.27 |
| MV17 | 10.10 | 80 | 18 | 0.57 | 7.4 | 7.1 | 1.0 | 84 | 41 | 80 | 11 | 105 | 113 | 400 | 0.01 | 5 | 50 |
| MV18 | 01.03 | 400 | 11 | 0.50 | nd | 7.5 | 0.4 | 22 | 11 | 43 | 4 | 92 | 59 | 37 | 1.2 | 0.29 | 3.3 |
| MV18 | 05.03 | 50 | 24 | 0.47 | nd | 7.4 | 0.9 | 39 | 19 | 104 | 10 | 135 | 175 | 56 | 0.13 | 0.08 | 0.25 |
| MV18 | 09.04 | 6 | 21 | 0.46 | nd | 7.6 | 1.0 | 45 | 22 | 110 | 15 | 150 | 170 | 100 | 0.06 | 0.12 | 0.60 |

**Table 2** continued

| No. | Date (mm.yy) | Flow (L/s) | pH | EC (mS) | Cd (μg/L) | Pb (μg/L) | Cu (μg/L) | Ni (μg/L) | Co (μg/L) | Al (μg/L) | As (μg/L) | Y (μg/L) | ΣREE (μg/L) | Ce* | Eu* | La/Gd ($_N$) | La/Yb ($_N$) |
|---|---|---|---|---|---|---|---|---|---|---|---|---|---|---|---|---|---|
| MV4 | 09.04 | 0.2 | 4.0 | 3.7 | 7,800 | 1,500 | 1,700 | 950 | 760 | 2,270 | 4.4 | 100 | 1,230 | 0.9 | 1.7 | 0.5 | 4.9 |
| MV4 | 09.08 | 0.1 | 4.2 | 4.0 | 9,000 | 1,800 | 1,800 | 1,200 | 800 | 2,200 | 8.0 | 140 | 1,470 | 0.9 | 1.7 | 0.5 | 4.6 |
| MV4 | 12.09 | 1 | 3.8 | 3.5 | 9,000 | 2,300 | 2,400 | 1,000 | 690 | 2,000 | 2.8 | 110 | 1,170 | 0.9 | 1.8 | 0.5 | 5.9 |
| MV4 | 03.10 | 1 | 4.1 | 3.0 | 12,000 | 3,200 | 3,400 | 1,200 | 800 | 8,900 | 0.7 | 84 | 1,090 | 1.0 | 2.2 | 0.6 | 6.4 |
| MV5 | 09.04 | 0.5 | 4.0 | 3.2 | 4,400 | 1,840 | 580 | 930 | 550 | 6,600 | 1.7 | 78 | 548 | 0.9 | 1.6 | 0.4 | 2.6 |
| MV5 | 09.08 | 0.3 | 3.4 | 2.9 | 3,800 | 2,200 | 550 | 790 | 460 | 6,000 | 3.1 | 76 | 497 | 0.9 | 1.6 | 0.4 | 2.6 |
| MV5 | 12.09 | 1 | 4.3 | 2.4 | 4,000 | 2,000 | 780 | 600 | 310 | 4,000 | 1.2 | 49 | 340 | 0.9 | 1.7 | 0.4 | 3.7 |
| MV5 | 03.10 | 2 | 6.5 | 1.7 | 2,300 | 820 | 570 | 500 | 270 | 4,200 | 0.4 | 19 | 180 | 0.9 | 1.9 | 0.8 | 7.6 |
| MV5 | 10.10 | 1 | 5.0 | 2.0 | 5,500 | 1,300 | 950 | 710 | 350 | 1,350 | 4.0 | 51 | 372 | 0.8 | 1.5 | 0.5 | 4.6 |
| MV6 | 12.09 | 4 | 4.3 | 2.6 | 4,800 | 1,800 | 850 | 760 | 440 | 3,000 | 3.5 | 83 | 854 | 0.9 | 1.6 | 0.7 | 7.4 |
| MV6 | 03.10 | 3 | 4.3 | 2.4 | 6,190 | 2,100 | 1,400 | 900 | 540 | 7,500 | 2.4 | 65 | 793 | 0.9 | 2.1 | 0.7 | 7.8 |
| MV6 | 10.10 | 3 | 5.4 | 1.5 | 1,370 | 725 | 210 | 480 | 280 | 194 | 2.8 | 49 | 459 | 1.0 | 2.1 | 0.8 | 9.0 |
| MV8 | 09.08 | 1.2 | 3.5 | 4.2 | 5,300 | 3,600 | 560 | 1,300 | 850 | 5,000 | 18 | 180 | 1,940 | 0.9 | 1.4 | 0.9 | 11.5 |
| MV9 | 09.08 | 0.01 | 6.0 | 3.5 | 230 | 1,070 | 7 | 850 | 440 | 2 | 260 | 25 | 134 | 0.7 | 1.5 | 1.3 | 13.7 |
| MV11 | 09.04 | 6 | 3.4 | 4.2 | 1,900 | 2,000 | 310 | 1,300 | 990 | 5,000 | 27 | 130 | 1,430 | 0.9 | 1.5 | 1.0 | 12.7 |
| MV11 | 09.08 | 1 | 3.3 | 4.0 | 2,000 | 2,100 | 220 | 1,300 | 680 | 2,000 | 6.6 | 90 | 891 | 0.9 | 1.6 | 0.8 | 9.4 |
| MV11 | 03.10 | 6 | 6.0 | 1.6 | 1,600 | 320 | 350 | 500 | 280 | 480 | 2.0 | 28 | 308 | 0.9 | 1.9 | 1.1 | 17.4 |
| MV12 | 09.04 | 1 | 3.3 | 4.2 | 1,500 | 1,900 | 280 | 1,200 | 880 | 4,900 | 15 | 115 | 1,300 | 0.9 | 1.5 | 1.0 | 12.5 |
| MV12 | 10.10 | 5 | 5.1 | 1.6 | 430 | 560 | 94 | 220 | 110 | 140 | 0.7 | 17 | 154 | 0.8 | 1.4 | 0.9 | 10.6 |
| MV13 | 09.04 | 10 | 3.3 | 3.9 | 1,300 | 2,800 | 250 | 1,100 | 630 | 4,000 | 3.3 | 83 | 904 | 0.9 | 1.5 | 0.9 | 10.0 |
| MV13 | 09.08 | 1 | 3.4 | 4.0 | 1,800 | 3,500 | 200 | 1,100 | 580 | 1,550 | 4.5 | 80 | 794 | 0.8 | 1.6 | 0.9 | 9.7 |
| MV13 | 03.10 | 7 | 6.2 | 1.4 | 1,100 | 570 | 170 | 380 | 190 | 500 | 1.1 | 12 | 148 | 0.8 | 1.8 | 1.4 | 19.7 |
| MV13 | 10.10 | 7 | 4.8 | 1.7 | 600 | 1,040 | 120 | 270 | 134 | 197 | 1.0 | 21 | 193 | 0.8 | 1.4 | 0.8 | 8.9 |
| MV14 | 09.04 | 2 | 3.6 | 3.8 | 1,300 | 3,300 | 360 | 1,100 | 610 | 5,000 | 2.8 | 100 | 953 | 0.9 | 1.6 | 0.9 | 9.8 |
| MV14 | 03.10 | 5 | 7.0 | 1.2 | 840 | 75 | 28 | 280 | 130 | 45 | 0.2 | 3.5 | 40 | 0.6 | 1.6 | 3.0 | 45.8 |
| MV15 | 09.04 | 1 | 6.2 | 3.7 | 2,000 | 500 | 110 | 1,200 | 410 | 8 | 2.3 | 65 | 551 | 0.5 | 1.3 | 1.9 | 24.3 |
| MV16 | 09.04 | 1 | 6.4 | 4.2 | 2,900 | 130 | 59 | 1,300 | 430 | 5 | 2.9 | 57 | 464 | 0.4 | 1.3 | 2.7 | 25.3 |
| MV16 | 10.10 | 50 | 6.4 | 1.7 | 1,040 | 170 | 30 | 440 | 113 | 4 | 1 | 14 | 113 | 0.5 | 1.3 | 1.8 | 19.0 |
| MV17 | 09.04 | 5 | 7.6 | 1.0 | 1.4 | 4.6 | 2.9 | 2.6 | 0.43 | 18 | 5 | 0.09 | 0.46 | 0.7 | 1.3 | 0.3 | 0.5 |
| MV17 | 10.10 | 80 | 7.1 | 1.0 | 169 | 3.6 | 7 | 110 | 16 | 4 | 1 | 0.31 | 1.4 | 0.4 | 1.0 | 1.4 | 3.3 |
| MV18 | 01.03 | 400 | 7.5 | 0.4 | 20 | 57 | 2.7 | 7.8 | 2.7 | 1,240 | 1 | 2.4 | 14 | 0.8 | 1.3 | 0.6 | 0.9 |
| MV18 | 05.03 | 50 | 7.4 | 0.9 | 0.9 | 9.5 | 1.8 | 2.4 | 0.63 | 9 | 3 | 0.09 | 0.35 | 0.8 | 2.1 | 0.4 | 0.2 |
| MV18 | 09.04 | 6 | 7.6 | 1.0 | 0.8 | 3.5 | 4.9 | 6.9 | 0.63 | 18 | 5 | 0.07 | 0.29 | 0.7 | 2.5 | 0.6 | 0.5 |

$Ce^* = Ce_N/(La_N + Pr_N)$; $Eu^* = 2Eu_N/(Sm_N + Gd_N)$; $_N$ = concentration of each REE in water normalized to the corresponding value in PAAS (McLennan 1989)

(about 50%) in $SO_4$, Zn, Cd, Cu, Fe, Mn, Ni, and Co concentrations in the MV4 drainage in 2010, compared with values recorded in 1996. In contrast, dissolved Al and Pb concentrations in 2010 were similar to levels in 1996.

## Impact of Mine Drainages on Surface Water

Mine drainages from Montevecchio are directly discharged into the Rio Montevecchio-Rio Sitzerri stream, which flows into the Marceddì Lagoon (Fig. 1). This stream also receives seeps (MV9 in Table 2) from the Piccalinna tailings (flow 0.1–0.3 L/s), and further downstream, input from uncontaminated tributaries, which vary widely in flow depending on rainfall.

Results derived from water sampling carried out under low flow conditions in September 2004 are compared with results derived from water sampling carried out under relatively high flow conditions in October 2010 (Figs. 4, 5, 6). Similar trends were observed when water sampling was repeated under similar flow conditions (see Table 2); thus, those data have been omitted in these plots.

Sulphate and metal concentrations in mine drainages at low flow are much higher than those observed at high flow. It should be noted that in September 2004, many tributaries

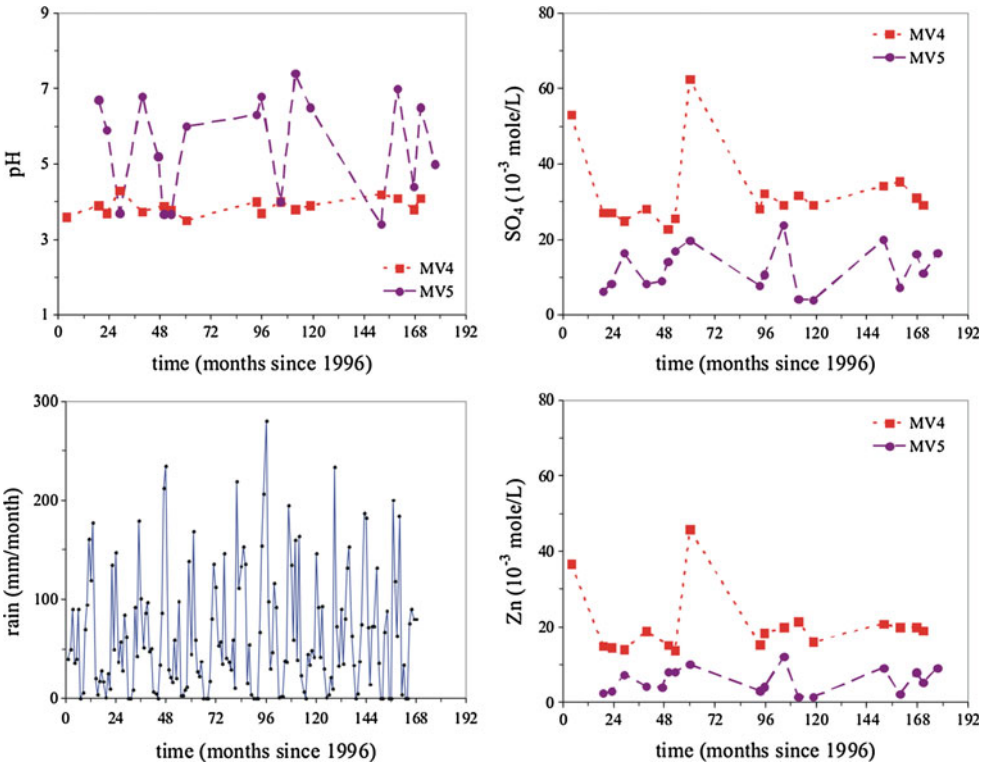


**Fig. 2** Temporal (1996–2010) variation of pH, sulphate, and zinc in the MV4 and MV5 adit waters and monthly precipitation in the Montevecchio area (sample locations are shown in Fig. 1)

were either dry or at low flow, so that the mine drainages supplied most of the water to the upper Rio Montevecchio stream.

Mine drainages at low flow were more acidic (pH 4, Fig. 4a) than at high flow (pH 5, Fig. 4b). In the stream, pH trends were similar under different seasonal conditions. The pH was lowest at about 2 km downstream of the mines, and at about 8 km, the pH rose above 6 and continued to increase downstream until reaching neutrality.

Removal of Fe, Al, and Pb from solution is related to pH trends. Iron precipitation occurred at relatively short (2 km) distance from the mine drainages (Fig. 5a-b), and was accompanied by a marked decrease in dissolved Zn (Fig. 4c–d), Cd (Fig. 4e–f), Cu (Fig. 6c–d), and As (not shown), which is in agreement with solids analysis (see Table 1). The acidity produced by Fe precipitation allowed Al (Fig. 5c) and Pb (Fig. 5e) to remain in solution for 4 km downstream in September 2004. Less acidic conditions in October 2010 favoured Al (Fig. 5d) and Pb (Fig. 5f) removal at shorter distances from the mines. The greatest decreases in sulphate, Zn, Cd, Ni, Mn, and REE concentrations occurred when tributaries that do not drain the mining area flowed into the stream.

REE concentrations in the studied waters reach values close to 2 mg/L. Slightly negative Ce and positive Eu anomalies (Ce* and Eu*, respectively, in Table 2) were observed. Figures 7a–b show dissolved REE concentrations versus distance from mine drainages. About 26% of the REE removal accompanies Fe precipitation; when about 60% of the REE was removed when both Fe and Al had precipitated. REE trends in the stream water match sulphate trends, which is consistent with the tendency of REE to form aqueous sulphate complexes in acid mine drainage (Verplanck et al. 2004). Drops in REE concentration might be due to sorption and/or dilution processes.

In Figs. 7c–d, each REE concentration in the water has been normalized to the corresponding concentration in post-Archean Australian shales (PAAS, McLennan 1989), which is considered a good analog of crustal materials. The resulting patterns in waters influenced by mine drainage show enrichment in light REE (LREE: La to Nd) with respect to heavy REE (HREE: Dy to Lu), as inferred from PAAS-normalized La/Yb values in the range of 2–46 (Table 2). Slight enrichment in middle REE (MREE: Sm to Tb) is observed in the acid waters ($E_{MREE} = 2.2$ in MV4; $E_{MREE}$ calculated by Pérez-López et al. 2010). Such enrichment has been reported in acid mine drainage at other mine sites and might be attributed to the weathering of sulphide minerals (e.g. Pérez-López et al. 2010 and references therein).

## Attenuation Processes

Attenuation of aqueous contaminants downstream of mine drainages under high flow condition appears to be driven by dilution from uncontaminated tributaries.

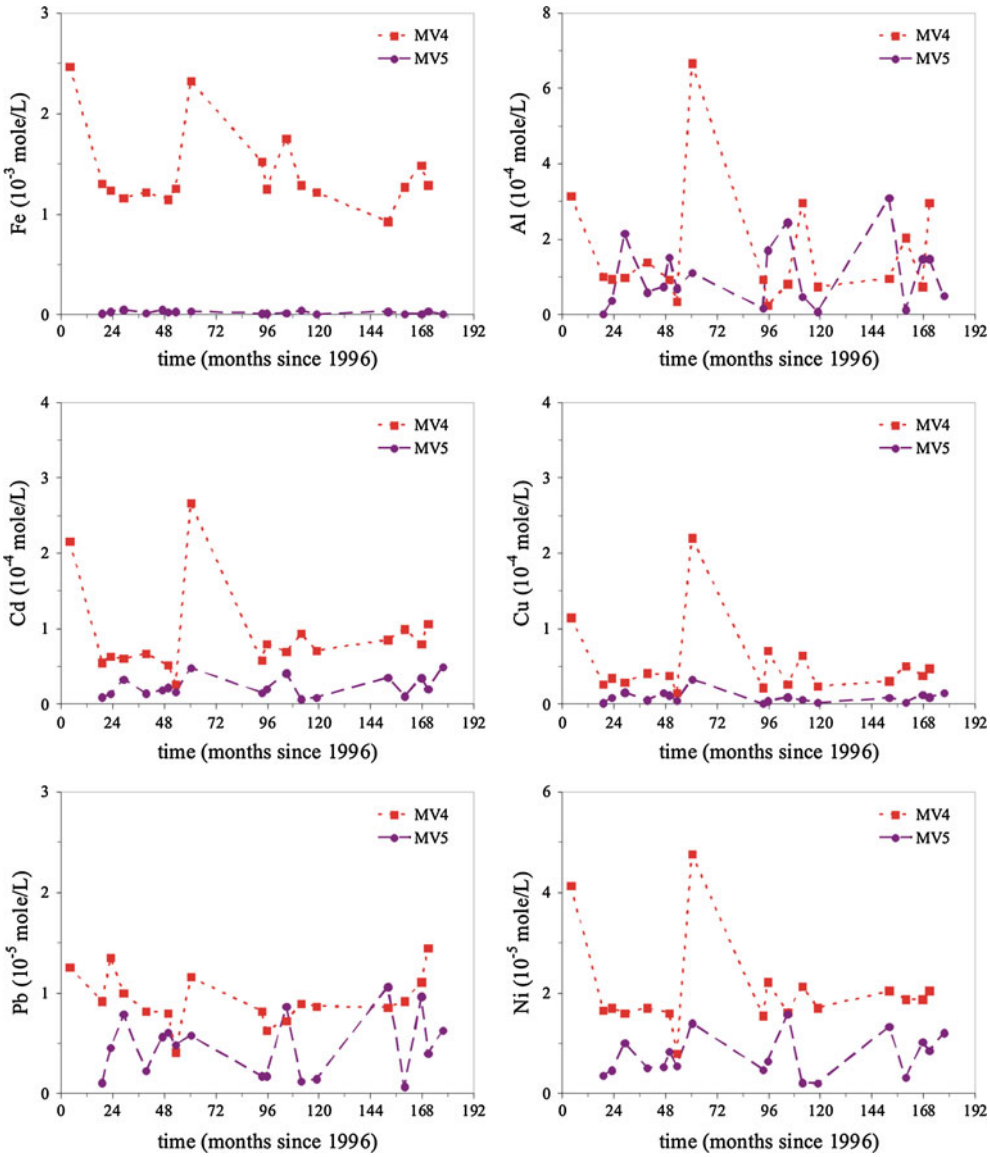


**Fig. 3** Temporal variation of iron, aluminum, cadmium, copper, lead, and nickel in the MV4 and MV5 adit waters at Montevecchio (sample locations are shown in Fig. 1)

Attenuation under low flow conditions might be a result of several processes. Summarizing, at 2 km downstream from where the mine drainage enters the stream, the water had a pH of 3.3; $1.8 \times 10^{-3}$ mol/L of Fe, $11 \times 10^{-3}$ mol/L of Zn, $7.3 \times 10^{-3}$ mol/L of $SO_4$, $5.7 \times 10^{-5}$ mol/L of Cd, and $0.4 \times 10^{-3}$ mol/L of $SiO_2$ had been removed. At 8 km downstream, the stream water (MV16) had a pH of 6.2; Al and Pb had been removed but sulphate (Fig. 4a), Zn (Fig. 4c), Cd (Fig. 4e), Ni (Fig. 6a), and Mn (see Table 2) persisted in the water at relatively high concentrations. At 12 km downstream, the Rio Sitzerri flow increases and concentrations of sulphate, Zn, Cd, Ni, Mn, REE, and other trace metals in water MV17 decreased.

To understand the sharp decrease in concentrations of several components observed between MV16 and MV17 in September 2004, geochemical processes were modelled using PHREEQC. Water MV16 was at equilibrium with gypsum, K-jarosite, and rhodochrosite, but was oversaturated with pyrolusite, amorphous Fe(III)-hydroxide, willemite, and hemimorphite (Table 3). Water MV17 was close to equilibrium with calcite and oversaturated with amorphous Fe(III)-hydroxide and hemimorphite (Table 3). These results do not explain the strong decrease in Ca, Mg, and $SO_4$, but might indicate precipitation of Mn with pyrolusite and Zn with hemimorphite or willemite. However, hemimorphite saturation indexes (SI) are too high (12.6 and 8.5, in MV16 and MV17 waters, respectively), which likely indicates that either hemimorphite does not precipitate or its $K_s$ value is unreliable.

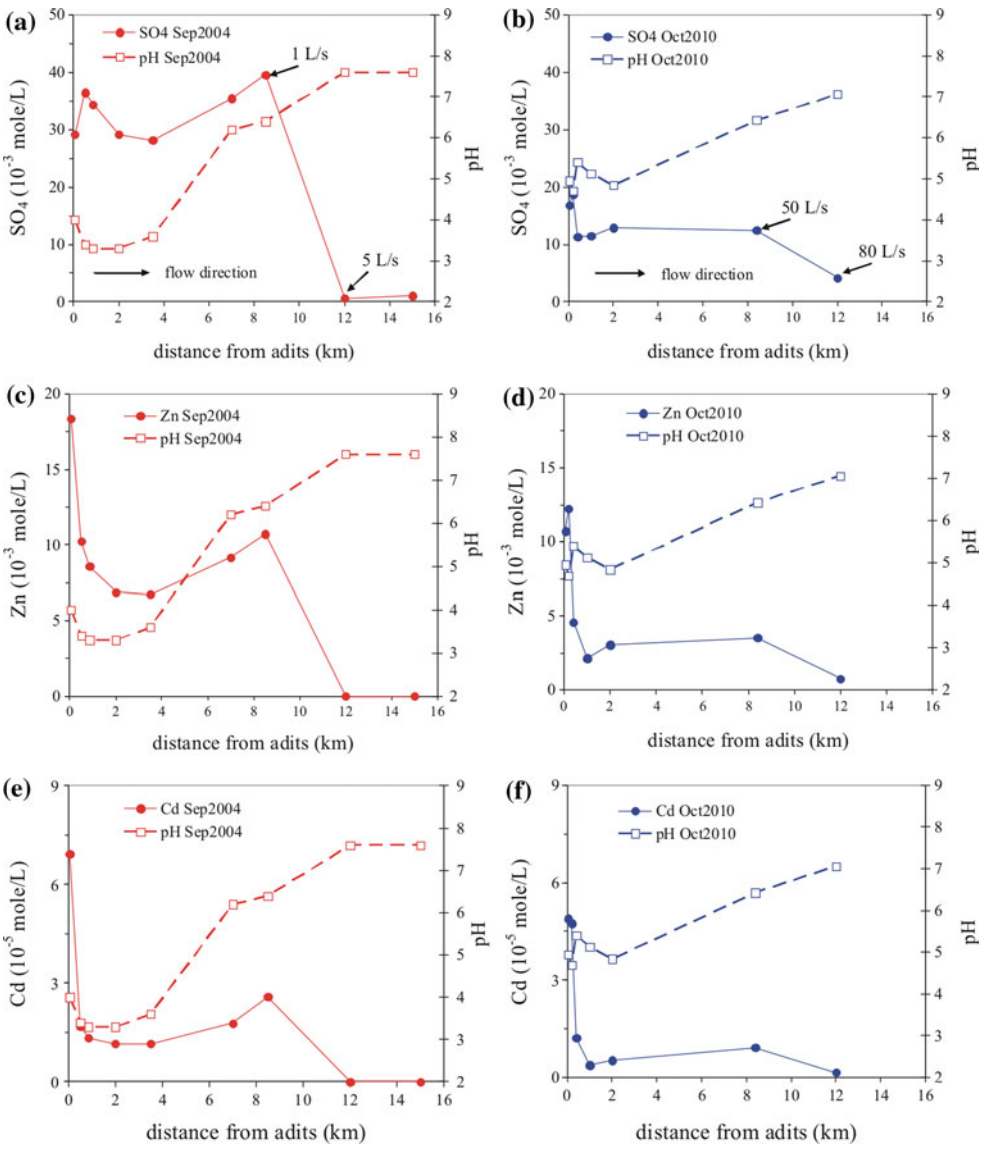


**Fig. 4** Variations of pH, dissolved sulphate, zinc, and cadmium in waters sampled along the Rio Montevecchio—Rio Sitzerri under low flow (**a**, **c**, **e**) and high flow (**b**, **d**, **f**) conditions

These observations suggest that the chemical composition of water MV17 is due to conservative mixing between MV16 and an unknown tributary (Tr, surface and/or groundwater) or that precipitation of solid phases has occurred due to evaporation and/or mixing.

## Conservative Mixing

Verification of the conservative mixing hypothesis is complicated because the Tr water responsible for the increased flow at site MV17 was not identified. This drawback was overcome by calculating the Tr chemical composition from Eq. 3:

$$x\ C_{MV16} + y\ C_{Tr} = (x + y) \cdot C_{MV17} \quad (3)$$

where x and y are flow rates (L/s) and C is the dissolved concentration of chemical components. In order to calculate $C_{Tr}$, the x value was fixed equal to 1 L/s (i.e. flow rate estimated at MV16) and the y value was varied from that estimated in the field (y = 4 L/s) to 99 L/s.

Figure 8 shows some results of conservative mixing simulations at increasing Tr flow rates. Negative concentrations in Fig. 8 indicate failure of conservative mixing. Elements Ca, Mg, Cu, and Li (as well as Pb) approach conservative mixing (concentration 'zero') at 15–25 L/s Tr flow rate and $SO_4$ at 60 L/s, but Zn, Mn, and Cd indicate a Tr flow rate >2,000 L/s. Taking into account uncertainties in flow rates estimated at MV16 and MV17, and that the dispersion of stream water MV16 over a nearly flat area might have altered the mixing ratio, a value of 20 L/s for Tr flow rate was assumed and used to calculate the Tr chemical composition since, on the basis of field observations, Tr flow rates higher than 20 L/s seem unrealistic. Negative concentration values in Fig. 8 can be used to

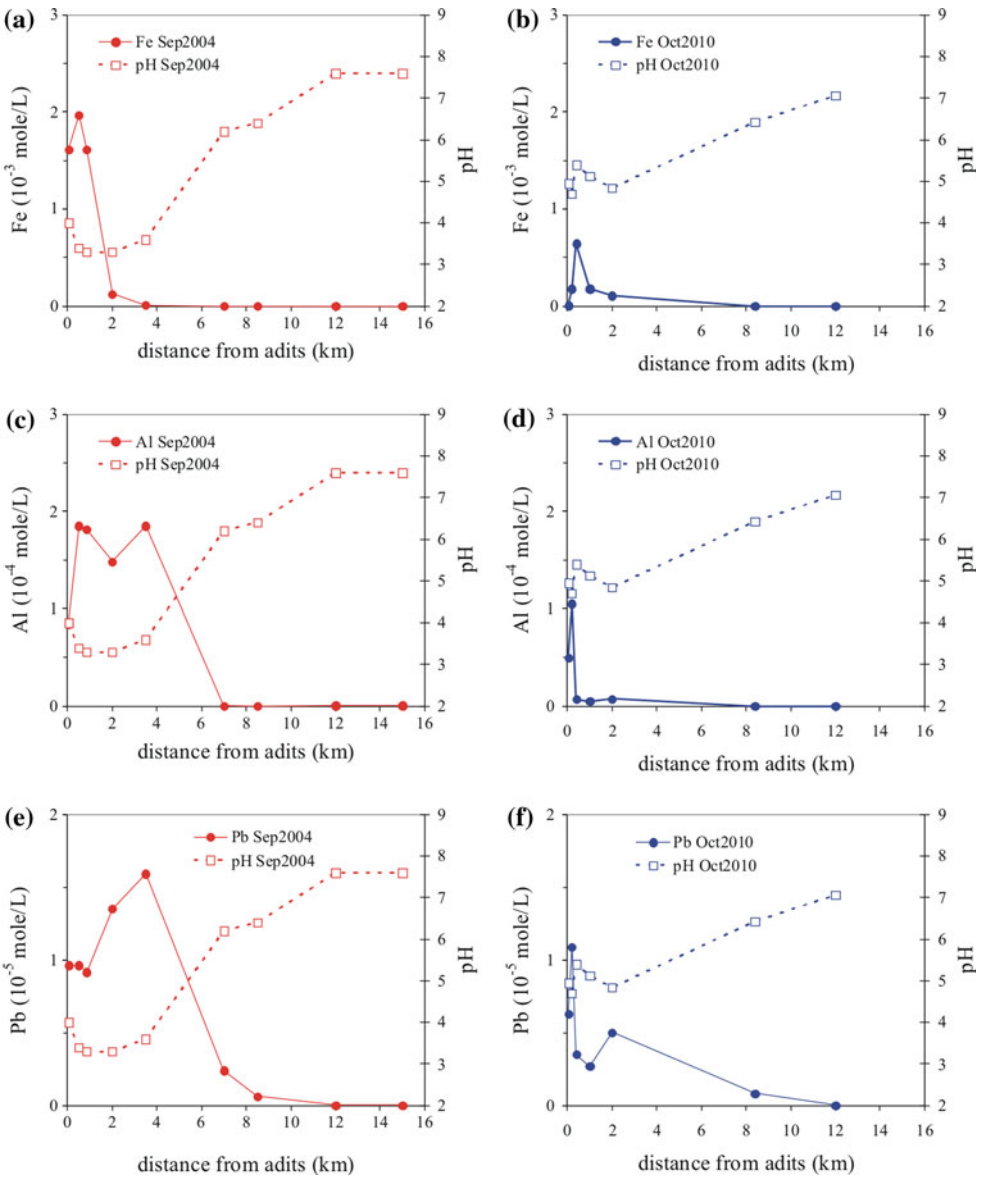


**Fig. 5** Variations of pH, iron, aluminum, and lead in waters sampled along the Rio Montevecchio – Rio Sitzerri under low flow (**a**, **c**, **e**) and high flow (**b**, **d**, **f**) conditions

calculate the extent to which the concentration in MV16 should decrease to obtain the measured concentration in MV17, assuming concentration 'zero' in Tr for each mixing ratio (Eq. 3).

Figure 9 shows calculated versus measured concentrations in MV17 using the mixing ratio MV16: Tr = 1:20. Most elements satisfy conservative mixing, but calculated Zn, Mn, Cd and Ni concentrations are much higher than those measured.

## Precipitation of Solid Phases

Simulation of conservative mixing, reported in column MV17[a] in Table 3, causes oversaturation with respect to hydrozincite, pyrolusite, rhodochrosite, smithsonite, and willemite. Therefore, these minerals were allowed to reach equilibrium by setting their SI values to zero. Taking into account that precipitation of mineral phases causes a pH decrease to 6.8, the pH was set to 7.6 by adding NaOH, resulting in a slight increase in Na. Amorphous Fe(III)-hydroxide and hemimorphite were excluded from equilibration constraints: the former because Fe satisfied conservative mixing (see Fig. 9) and Fe concentration in MV16 is so low that its precipitation would not affect concentrations of non-conservative components such as $SO_4$, Zn, and Mn; the latter because its oversaturation appears unrealistic.

Columns MV17[b] and MV17[c] in Table 3 show the results of equilibration with and without the constraint of chalcedony

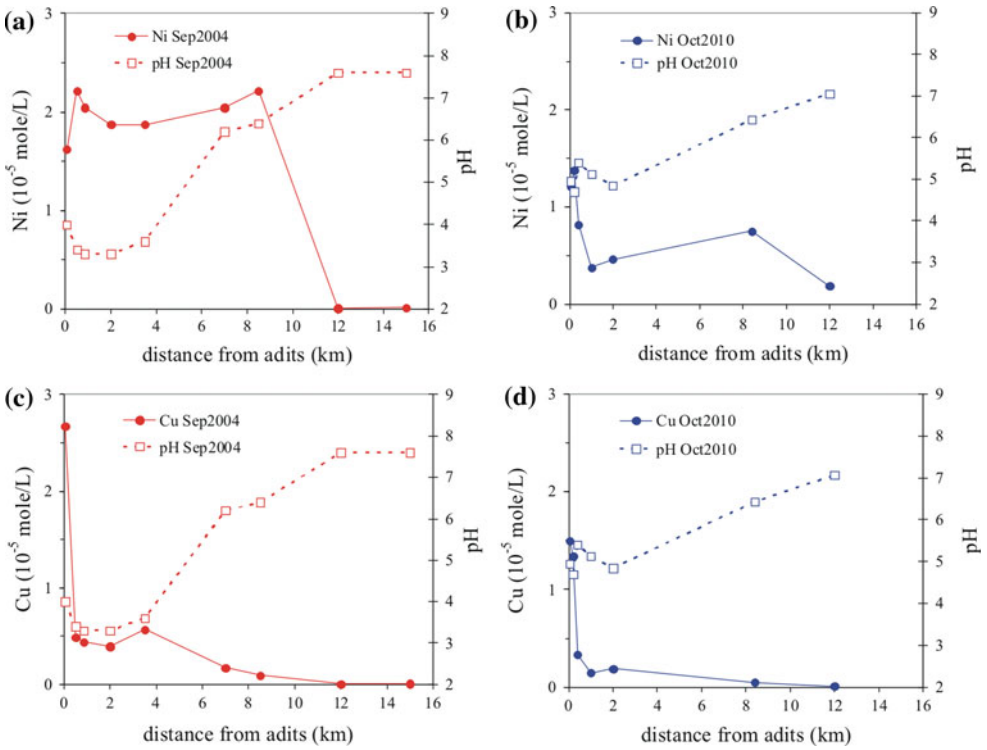


**Fig. 6** Variations of pH, nickel, and copper in waters sampled along the Rio Montevecchio – Rio Sitzerri under low flow (**a**, **c**) and high flow (**b**, **d**) conditions

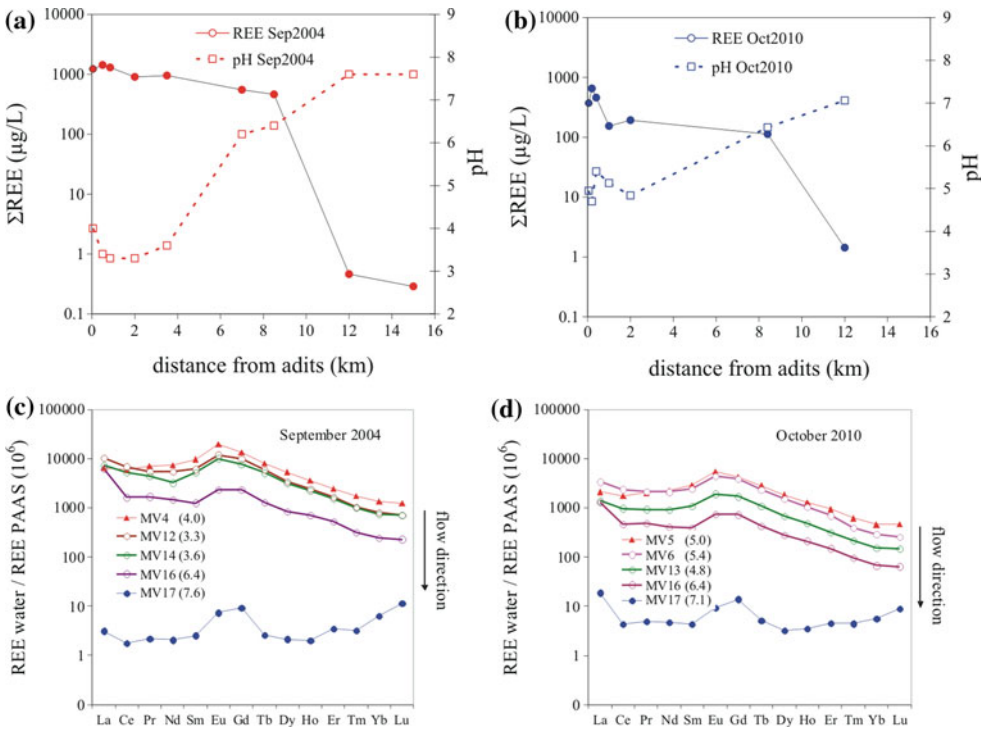


**Fig. 7** Variations of REE (La to Lu) and PAAS-normalized REE patterns in waters sampled along the Rio Montevecchio – Rio Sitzerri under low flow (**a**, **c**) and high flow (**b**, **d**) conditions; in **c**) and **d**), pH values are reported in parenthesis

saturation, respectively. In MV17[b], hydrozincite (53 mg/L) and rhodochrosite (11 mg/L) are precipitated together with traces of pyrolusite. In MV17[c], willemite (46 mg/L), rhodochrosite (11 mg/L), and hydrozincite (8 mg/L) are precipitated together with traces of pyrolusite. In both cases, Zn and Mn concentrations are still an order of magnitude higher than those measured in MV17, and $SO_4$ is three times higher.

**Table 3** Results of PHREEQC mixing between MV16 and Tr to obtain MV17

| Solution | MV16 | Tr | MV17 | MV17[a] | MV17[b] | MV17[c] |
|---|---|---|---|---|---|---|
| pH | 6.4 | 8.6 | 7.6 | 7.6 | 7.6 | 7.6 |
| pe | 10.7 | 7.9 | 7.9 | 9.1 | 8.6 | 8.6 |
| T °C | 24 | 21 | 21 | 21 | 21 | 21 |
| Ca | 550 | 9.2 | 35 | 35 | 35 | 35 |
| Mg | 320 | 0.80 | 16 | 16 | 16 | 16 |
| Na | 150 | 95 | 98 | 98 | 115 | 119 |
| K | 25.1 | 11.8 | 12.4 | 12.4 | 12.4 | 12.4 |
| Alkalinity | 12 | 136 | 130 | 130 | 104 | 114 |
| Cl | 160 | 129 | 130 | 130 | 130 | 130 |
| $SO_4$ | 3,800 | 0 | 61 | 182 | 182 | 182 |
| Si | 23 | 5.4 | 6.3 | 6.3 | 6.3 | 0.46 |
| Fe | 0.05 | 0.07 | 0.07 | 0.07 | 0.07 | 0.07 |
| Mn | 120 | 0 | 0.03 | 5.7 | 0.34 | 0.32 |
| Zn | 700 | 0 | 0.27 | 33.5 | 1.8 | 1.8 |
| Cd | 2,900 | 0 | 1.4 | 139 | 139 | 139 |
| Pb | 130 | 0 | 4.6 | 6.2 | 6.2 | 6.2 |
| Cu | 59 | 0.09 | 2.9 | 2.9 | 2.9 | 2.9 |
| Ni | 1,300 | 0 | 2.6 | 62 | 62 | 62 |
| Al | 5 | 18.7 | 18 | 18 | 18 | 18 |
| As | 2.9 | 5.1 | 5.0 | 5.0 | 5.0 | 5.0 |
| Li | 86 | 2.2 | 6.2 | 6.2 | 6.2 | 6.2 |
| B | 170 | 265 | 260 | 260 | 260 | 260 |
| Rb | 25 | 7.3 | 8.1 | 8.1 | 8.1 | 8.1 |
| Sr | 1,600 | 172 | 240 | 241 | 241 | 241 |
| Ba | 34 | 31 | 31 | 31 | 31 | 31 |
| SI Anglesite | −1.4 | | −5.05 | −4.39 | −4.37 | −4.40 |
| SI Bianchite | −2.98 | | −7.46 | −4.93 | −6.17 | −6.18 |
| SI Calcite | −1.94 | 0.18 | −0.29 | −0.42 | −0.43 | −0.40 |
| SI Cerrusite | −1.92 | | −1.75 | −1.63 | −1.63 | −1.63 |
| SI Chalcedony | 0.49 | −0.14 | −0.05 | −0.06 | −0.06 | −1.19 |
| SI Epsomite | −2.45 | | −4.63 | −4.23 | −4.22 | −4.22 |
| SI $Fe(OH)_3$(am) | 0.98 | 1.88 | 1.90 | 1.89 | 1.89 | 1.89 |
| SI Goslarite | −2.78 | | −7.23 | −4.70 | −5.94 | −5.95 |
| SI Gypsum | 0.02 | | −2.10 | −1.70 | −1.68 | −1.68 |
| SI Hydrozincite | −0.42 | | −3.96 | 6.19 | 0.00 | 0.00 |
| SI K-jarosite | 0.04 | | −3.91 | −3.01 | −3.02 | −3.02 |
| SI Pyrolusite | 2.19 | | −2.43 | 2.26 | 0.00 | 0.00 |
| SI Rhodochrosite | −0.08 | | −0.94 | 1.23 | 0.00 | 0.00 |
| SI Otavite | −1.2 | | −1.60 | 0.26 | 0.24 | 0.28 |
| SI Smithsonite | −0.61 | | −1.33 | 0.66 | −0.60 | −0.58 |
| SI Willemite | 1.79 | | −0.52 | 3.61 | 1.16 | 0.00 |
| SI Hemimorphite | 12.61 | | 8.49 | 16.71 | 11.83 | 9.50 |
| Hydrozincite prec. | | | | | 53 | 8 |
| Pyrolusite prec. | | | | | tr | tr |
| Rhodochrosite prec. | | | | | 11 | 11 |
| Willemite prec. | | | | | | 46 |

MV16 and MV17 refer to measured values; Tr refers to the hypothetical tributary calculated for a mixing ratio MV16:Tr = 1:20; column MV17[a] is calculated for conservative mixing; columns MV17[b] and MV17[c] are calculated from MV17[a] after mineral equilibration with and without the constraint of chalcedony saturation, respectively. Concentrations are expressed in mg/L from Ca to Zn and in μg/L from Cd to Ba; amounts of precipitated minerals are expressed in mg/L

*SI* saturation index, *tr* traces

Concentrations of Cd and Ni are not affected by PHREEQC simulations (see Table 3) because they do not easily form pure minerals but are preferentially incorporated in Zn-Mn phases (see Table 1).

The performed simulations were also tested by taking into account the strong supersaturation in hemimorphite and allowing equilibration but the results were not significantly different from those described above. Analogous results were also obtained when 76% MV16 water was allowed to evaporate prior to conservative mixing (mixing ratio MV16: Tr = 0.24: 4.76 = 0.05) and subsequent equilibration.

On the basis of PHREEQC simulations, conservative mixing and precipitation cannot fully explain the sharp decrease of $SO_4$, Zn, Cd, Mn, and Ni observed between MV16 and MV17. However, the Zn-Mn-$SO_4$ composition of efflorescence materials (see Table 1) suggests that during the dry season, the underground inflow of MV16 water, combined with evaporation and mixing with dilute surface and/or ground water, might explain the strong decrease of dissolved Zn, Mn, and $SO_4$ concentrations observed at MV17.

## Conclusions

High contamination levels persist in the Montevecchio mine drainages after 15 years of flushing. Contaminated mine drainages flow directly into the Rio Montevecchio—Rio Sitzerri stream. Decreasing trends of sulphate and metals in the stream water depend on the contribution of runoff and tributaries to the stream. Attenuation in the dissolved load of contaminants occurs by precipitation of solid phases and by dilution via uncontaminated tributaries and rainwater. In the stream water, Fe, Al, and Pb are removed at relatively close (2–4 km) distances from the mine discharges. Some elements, such as As, appear to be co-precipitated or adsorbed on the hydrated iron oxide (ochre). The dispersion of Zn, Cd, Mn, Ni, and REE extends further downstream, especially during low flow conditions.

Despite natural attenuation in dissolved contaminants, the estimated amount of dissolved metals discharged daily into the Marceddì Lagoon is significant, especially when stream flow rises dramatically after storm events. In fact, concentrations of Zn, Cd, and Pb in the stream water increase under high runoff conditions, due to erosion and weathering of the exposed mining-related residues and the dissolution of efflorescent salts. Under such conditions, the downstream dispersion of contaminants is favoured by transport via adsorption processes onto very fine particles (<0.4 μm) and/or associated with colloids.

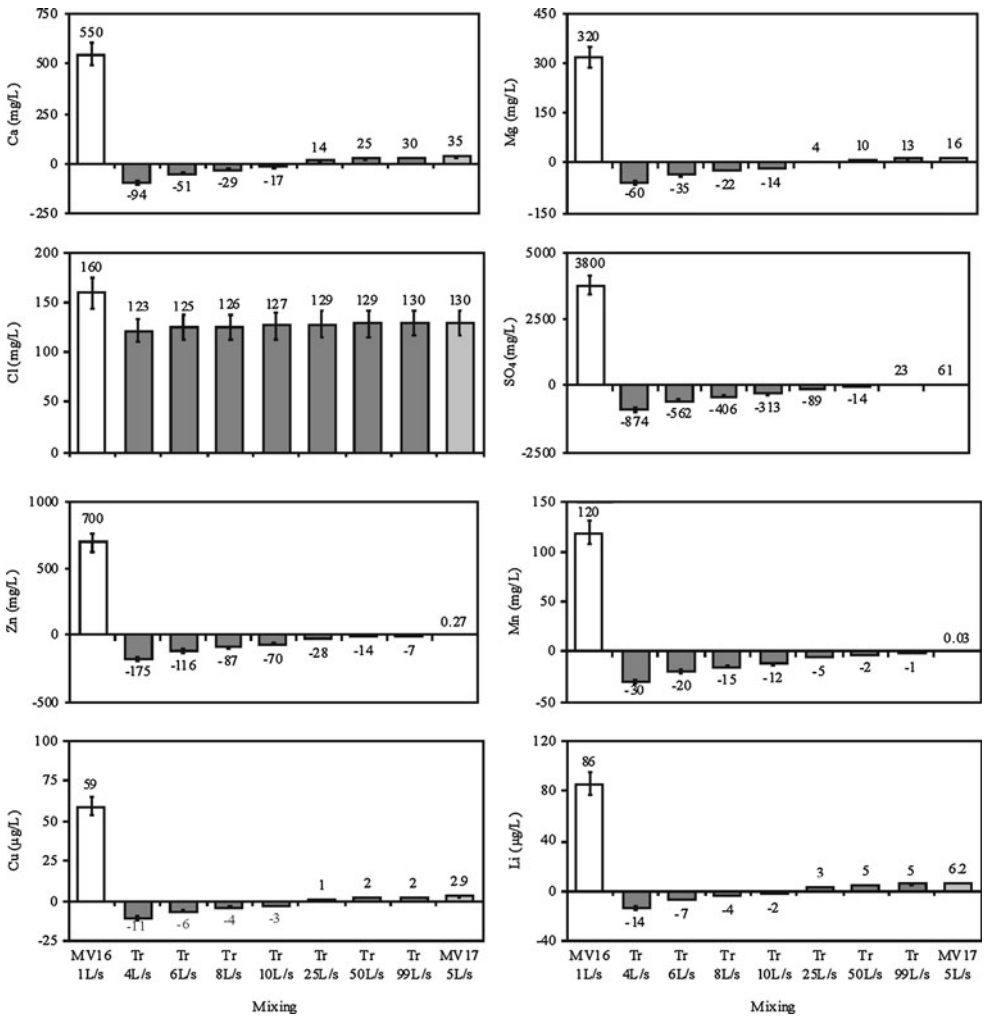


**Fig. 8** Concentrations of dissolved components calculated for conservative mixing between water MV16 and tributary Tr to obtain MV17. The MV16 and MV17 flow rates (1 L/s and 5 L/s, respectively) were estimated on site; the Tr flow rate varies from 4 to 99 L/s. Error bars of 10% are reported. A negative concentration indicates failure of conservative mixing for the corresponding Tr flow rate

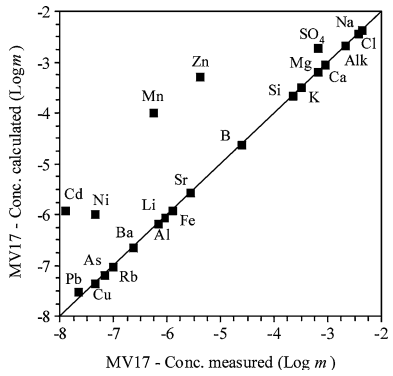


**Fig. 9** Results of conservative mixing performed with PHREEQC for a mixing ratio MV16:Tr = 1:20 to obtain MV17. Calculated concentrations are compared with measured concentrations, both expressed in log molality. The equivalence satisfies conservative mixing

**Acknowledgments** Authors thank the EU (Umbrella project, FP7 no. 226870), the University of Cagliari, and the Fondazione Banco di Sardegna for financial support. Thanks to Dr. D.C. "Bear" McPhail (Research School of Earth Sciences, Australian National University, Canberra, Australia) for providing the hemimorphite solubility constant.

## References

Berger AC, Bethke CM, Krumhansl JL (2000) A process model of natural attenuation in drainage from a historic mining district. Appl Geochem 15:655–666

Biddau M (1978) Indagine chimica-idrologica sulle possibilità di utilizzazione delle acque edotte nel Sulcis-Iglesiente. La Programmazione in Sardegna 67(68):99–115 in Italian

Bigham JM, Schwertmann U, Traina SJ, Winland RL, Wolf M (1996) Schwertmannite and the chemical modeling of iron in acid sulphate waters. Geochim Cosmochim Acta 60(12):2111–2121

Caboi R, Cidu R, Fanfani L, Zuddas P (1996) Abandoned mine sites: implications for water quality. In: Ciccu R (ed) Proc, SWEMP 96, vol 2. DIGITA Univ of Cagliari, Italy, pp 797–805

Chapman BM, Jones DR, Jung RF (1983) Processes controlling metal ion attenuation in acid mine drainage stream. Geochim Cosmochim Acta 47:1957–1973

Cherry DS, Currie RJ, Soucek DJ, Latimer HA, Trent GC (2001) An integrative assessment of a watershed impacted by abandoned mined land discharges. Environ Poll 111:377–388

Da Pelo S (1998) Mineralogia e geochimica ambientale di aree minerarie attive e dismesse. PhD Thesis, Univ di Cagliari (in Italian), Cagliari, Italy

Da Pelo S, Corsini F, Lattanzi P, Parrini P Zuddas P (1996) Mineralogia e geochimica degli sterili di flottazione nell'area mineraria di Montevecchio, Sardegna: dati preliminari. In:

Tanelli G (ed) Proc, Le proprietà dei minerali e le loro applicazioni alle problematiche ambientali, culturali e industriali, 1° incontro scientifico nazionale, vol 1. University of Modena, Italy, pp 33–35 (in Italian)

Dold B, Fontboté L (2001) Element cycling and secondary mineralogy in porphyry copper tailings as a function of climate, primary mineralogy and mineral processing. J Geochem Explor 74:3–55

Gandy CJ, Younger PL (2007) Predicting groundwater rebound in the South Yorkshire Coalfield, UK. Mine Water Environ 26:70–78

Hudson-Edwards KA, Macklin M, Curtis C, Vaughan D (1996) Processes of formation and distribution of Pb-, Zn-, Cd-, and Cu-bearing minerals in the Tyne Basin, northeast England: implications for metal-contaminated river systems. Environ Sci Technol 30:72–80

Kimball BA, Bianchi F, Walton-Day K, Runkel RL, Nannucci M, Salvadori A (2007) Quantification of changes in metal loading from storm runoff, Merse River (Tuscany, Italy). Mine Water Environ 26:209–216

Lim H-S, Lee J-S, Chon H-T, Sager M (2008) Heavy metal contamination and health risk assessment in the vicinity of the abandoned Songcheon Au–Ag mine in Korea. J Geochem Explor 96:223–230

McLennan SM (1989) Rare earth elements in sedimentary rocks: influence of provenance and sedimentary processes. In: Lipin BR, McKay GA (eds) Geochemistry and Mineralogy of Rare Earth Elements, Rev Mineral, vol 21. Mineralogical Society of America, Washington, DC, USA, pp 169–199

Navarro MC, Pérez-Sirvent C, Martínez-Sánchez MJ, Vidal J, Tovar PJ, Bech J (2008) Abandoned mine sites as a source of contamination by heavy metals: a case study in a semi-arid zone. J Geochem Exploration 96:183–193

Nordstrom DK (2009) Acid rock drainage and climate change. J Geochem Exploration 100:97–104

Nordstrom DK, Alpers CN (1999) Negative pH, efflorescent mineralogy, and consequences for environmental restoration at the Iron Mountain Superfund site, California. P Natl Acad Sci USA 96:3455–3462

Parkhurst DL, Appelo CAJ (1999) User's guide to PHREEQC (version 2)—a computer program for speciation, batch-reaction, one-dimensional transport, and in-verse geochemical calculations. USGS Water-Resources Investigations Report 99-4259, Denver, CO, USA

Pérez-López R, Delgado J, Nieto JM, Márquez-García B (2010) Rare earth element geochemistry of sulphide weathering in the São Domingos mine area (Iberian Pyrite Belt): a proxy for fluid–rock interaction and ancient mining pollution. Chem Geol 276:29–40

Ren HY, Zhuang DF, Singh AN, Pan JJ, Qiu DS, Shi RH (2009) Estimation of As and Cu contamination in agricultural soils around a mining area by reflectance spectroscopy: a case study. Pedosphere 19:719–726

Stumm W, Morgan JJ (1996) Aquatic Chemistry. 3rd Edit, John Wiley & Sons, NY

Verplanck PL, Nordstrom DK, Howard E, Taylor HE, Kimball BA (2004) Rare earth element partitioning between hydrous ferric oxides and acid mine water during iron oxidation. Appl Geochem 19:1339–1354

Wolkersdorfer C, Bowell R (eds) (2005) Contemporary reviews of mine water studies in Europe. Mine Water Environ 24: Supplement

Yu JY, Heo B, Choi IK, Cho JP, Chang HW (1999) Apparent solubilities of schwertmannite and ferrihydrite in natural stream waters polluted by mine drainage. Geochim Cosmochim Acta 63:3407–3416